Suppressed Blinking Dynamics of Single QDs on ITO

Shengye Jin, Nianhui Song, and Tianquan Lian*

Department of Chemistry, Emory University, Atlanta, Georgia 30322

ARTICLE

ABSTRACT The exciton quenching dynamics of single CdSe/$CdS_{3ML}ZnCdS_{2ML}ZnS_{2ML}$ core/multishell QDs adsorbed on glass, In_2O_3, and ITO have been compared. Single QDs on In_2O_3 show shorter fluorescence lifetimes and higher blinking frequencies than those on glass because of interfacial electron transfer from QDs to In_2O_3. Compared to glass and In_2O_3, single QDs on ITO show suppressed blinking activity as well as reduced fluorescence lifetimes. For QDs in contact with the n-doped ITO, the equilibration of their Fermi levels leads to the formation of negatively charged QDs. In these negatively charged QDs, the off states are suppressed because of the effective removal of the valence band holes, and their fluorescence lifetimes are shortened because of exciton Auger recombination and hole transfer processes involving the additional electrons. This study shows that the blinking of single QDs can be effectively suppressed on the surface of ITO. This phenomenon may also be observable for other QDs and on different n-doped semiconductors.

KEYWORDS: CdSe/$CdS_{3ML}ZnCdS_{2ML}ZnS_{2ML}$ core/multishell QDs · single QD · charged QDs · suppressed blinking dynamics · interfacial electron transfer · Auger relaxation

The fluorescence and interfacial charge transfer properties of colloidal semiconductor quantum dots (QD) are essential for their many applications, such as light-emitting diodes[1,2] and solar cells.[3−5] Single QDs on inert substrates exhibit strong intermittence in fluorescence intensity (known as "blinking").[6−33] The blinking activity is attributed to the photoinduced charging of QDs by electron transfer (ET) to trap states in QDs and the surrounding matrix and has been considered as an undesirable property in many applications. There have been many efforts to design novel QD structures and schemes for suppressing the blinking activity.[26−34] More recently, how the blinking dynamics affect the ET activity of single QDs has also been investigated.[35−37] The blinking activity was found to lead to intermittent ET dynamics for single QDs on TiO_2[36] and adsorbed with electron acceptors.[35,37] It remains unclear how the fluorescence property of single QDs is affected under device environment, in which QDs may be charged and interfacial charge transfer processes are active. For example, a recent ensemble average measurement has shown that, under external bias, QDs can be charged and their exciton lifetimes can be greatly reduced.[38] An important component of many QD-based devices is the interface between QDs and the conducting transparent electrodes, such as tin-doped indium oxide (ITO). Because the conduction band edge of ITO is lower than that of QDs, photoinduced interfacial ET from QDs to ITO is energetically allowed. Furthermore, as an n-doped semiconductor, the Fermi level in ITO is near its conduction band edge and higher than that of a neutral QD. When these materials are in contact, the equilibration of their Fermi levels leads to the formation of negatively charged QDs. Both the formation of charged particles and the presence of interfacial electron transfer pathways will likely affect the fluorescence lifetime and blinking activity of the QDs. To investigate these effects, we have studied exciton quenching dynamics of single QDs adsorbed on an ITO-coated coverslip and compared them with those on glass and In_2O_3 nanocrystalline thin films. We report here that, for single QDs on ITO, their exciton lifetimes are significantly shortened and their blinking activities are dramatically suppressed. We discuss the possible origins of the observed phenomenon.

RESULTS AND DISCUSSION

The fluorescence intensity and lifetime trajectories were recorded for 47, 45, and 50 single CdSe/$(CdS)_{3ML}(ZnCdS)_{2ML}(ZnS)_{2ML}$ core/multishell QDs on ITO, glass, and In_2O_3, respectively. Figure 1 shows typical fluorescence intensity and lifetime trajectories of

*Address correspondence to tlian@emory.edu.

Received for review December 11, 2009 and accepted February 09, 2010.

Published online February 19, 2010.
10.1021/nn901808f

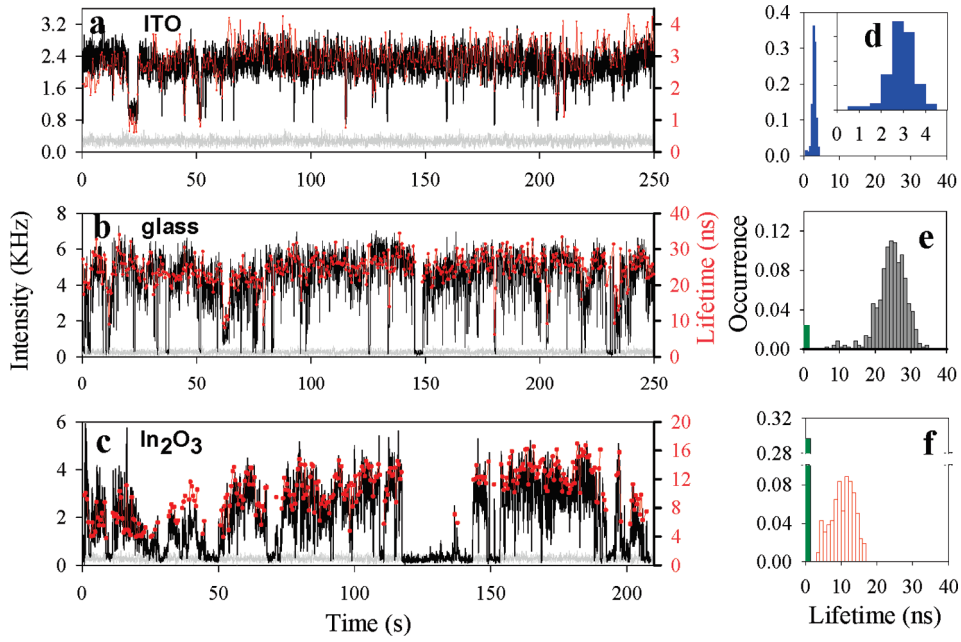

Figure 1. Typical fluorescence intensity (black) and lifetime (red) trajectories of single QDs on (a) ITO, (b) glass, and (c) In_2O_3. The gray trajectories indicate the background levels. The lifetime histograms of the QDs in a, b, and c are plotted in panels d, e, and f, respectively. In panel d, an expanded view of the data at short lifetimes is shown in the inset. Green bars in panels e and f indicate the occurrence of points with background intensity levels, for which the lifetime is assumed to be <0.25 ns.

single QDs on these substrates. The remaining trajectories for single QDs on ITO and In_2O_3 are shown in Figures S3 and S4 (Supporting Information). Intensity trajectories, that is, count rates as a function time, were constructed by binning the detected photons within a 50 ms window. The delay time histograms constructed from photons within a 0.5 s bin time were fitted to a single exponential decay to obtain their lifetimes along the trajectories. A representative histogram and its single exponential fit are shown in Figure S5. Compared with QDs on glass and In_2O_3, single QDs on ITO show very different intensity and lifetime trajectories. First, the blinking activity of the QD on ITO is significantly suppressed. Fluorescence intermittence is a common property of single QDs.[7−31] For example, single QDs on glass (Figure 1b) and In_2O_3 (Figure 1c and Figure S4) show strong fluorescence fluctuation between low intensity (background, off state) and a high intensity level (on state). However, for QDs on ITO (Figure 1a and Figure S3), the occurrence of blinking events is significantly reduced and the duration of the off state is shortened. For QDs on all substrates, the decrease of fluorescence intensity is accompanied by the reduction of lifetime, indicating a fluctuation in the nonradiative decay rate. Second, the lifetime of the QD on ITO is significantly shortened compared to those on glass and In_2O_3. The single QD on glass shown in Figure 1b has a broad on-state lifetime distribution centered at 23 ns. There are also events with intensity at the background level whose lifetimes cannot be accurately determined due to low count rates and were assumed to be <0.25 ns. However, for the QD on ITO (Figure 1a,d), the lifetime distribution is shifted to much shorter lifetimes (with a peak at 3 ns) and becomes much narrower than those for QDs on glass and In_2O_3.

To compare the ensembles of single QDs on different substrates, we have constructed the total fluorescence lifetime (Figure 2a−c) and intensity (Figure 2d−f) distributions by adding up histograms of single QDs. The total lifetime distribution of QDs on glass shows an off-state peak (events with background fluorescence intensity level and estimated lifetimes <0.25 ns) and a broad on-state peak centered at ~22 ns. For QDs on In_2O_3, the on-state distribution is shifted to shorter lifetimes with a peak at ~14 ns and the amplitude of the off state is increased. For QDs on ITO, their on-state lifetime distribution is centered at ~2.5 ns and becomes much narrower. Furthermore, the amplitude of off states becomes negligible. Because of the correlated change of fluorescence intensity and lifetime, a corresponding trend is also observed in the total fluorescence intensity distributions on these substrates. The total intensity histogram of QDs on glass shows broad distribution and two peaks for the on and off states. The on-state distribution is broad with a peak at a count rate of ~4 kHz (4000 counts per second), and the off-state peak is centered at ~400 Hz (background). For QDs on In_2O_3, the amplitude of the off-state peak becomes much larger and there is no apparent peak position in the on-state intensity distribution. The intensity histogram of QDs on ITO shifts to lower intensity levels with a peak centered at ~2 kHz. The distribution becomes much narrower, and there is negligible ampli-

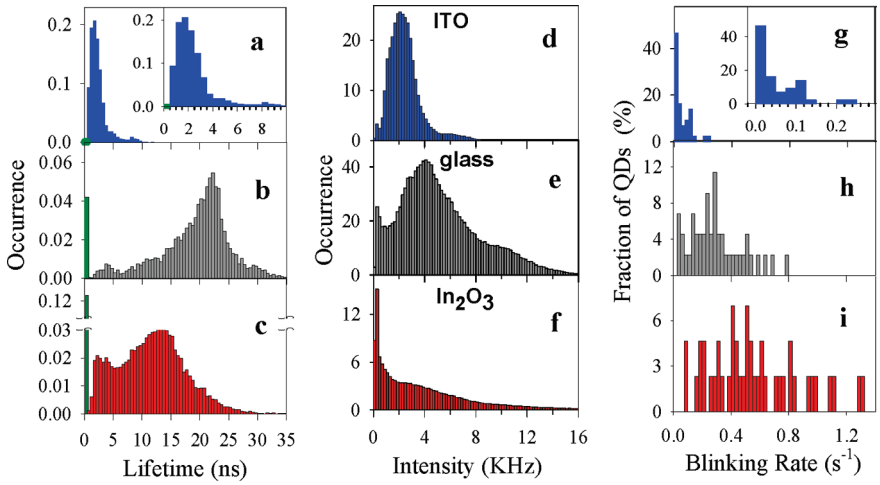

Figure 2. Comparison of lifetime and intensity distribution and fluctuation of single QDs on different substrates (47 on ITO, 45 on glass, and 50 on In_2O_3). Left panels: histograms of lifetime trajectories of all single QDs on (a) ITO, (b) glass, and (c) In_2O_3. The green bars indicate the occurrence of low intensity points along the trajectories, for which the lifetimes have been assumed to be <0.25 ns. Middle panels: histograms of the fluorescence intensity of all studied singe QDs on (d) ITO, (e) glass, and (f) In_2O_3. Right panels: histograms of blinking rate for single QDs on (g) ITO, (h) glass, and (i) In_2O_3. In panels a and g, expanded views of the data are shown in the inset.

tude of state, indicating again the suppression of blinking activities.

To compare the blinking activities of single QDs on different substrates, we have calculated the blinking frequency (number of blinking events per second over 180 s long trajectories) for all measured single QDs. The threshold fluorescence intensity, I_{Th}, separating the on and off states is defined as

$$I_{Th} = I_{av} + 3\sigma \quad (1)$$

where I_{av} is the average fluorescence intensity of the background and σ is its standard deviation. A blinking event is defined as a transition between the on and off states. The histograms of blinking frequency for single QDs on ITO, glass, and In_2O_3 are compared in Figure 2g−i, respectively. For QDs on glass, the blinking frequency is broadly distributed with an average value of 0.30 Hz. On In_2O_3, the single QDs blink more rapidly with an average frequency of 0.56 Hz. However, for QDs on ITO, the average blinking frequency is dramatically reduced to 0.05 Hz and 95% of QDs have a blinking frequency of less than 0.14 Hz.

As another way to compare the blinking dynamics of QDs on different substrates, we have calculated the on- and off-state probability densities $P_i(t)$ of single QDs according to the following definition:[14]

$$P_i(t) = \frac{N_i(t)}{N_{i,\text{total}}} \times \frac{1}{\Delta t_{i,\text{av}}} \quad (i = \text{on or off}) \quad (2)$$

where $N_i(t)$ is the number of on or off events of duration time of t, $N_{i,\text{total}}$ is the total number of on or off events, and $\Delta t_{i,\text{av}}$ is the average of the time intervals to the preceding and following events. As shown in Figure 3a,b, $P_{on}(t)$ and $P_{off}(t)$ of single QDs on different substrates show a power law distribution at short time but deviate from this distribution at long time tails, similar to those reported in the literature.[7,36,37,39−41] These $P(t)$ distributions can be fit by a truncated power law:[18,20−22,39]

$$P_i(t) = B_i t^{-m_i} \exp(-\Gamma_i t) \quad (i = \text{on or off}) \quad (3)$$

where B is the amplitude, m the power law exponent,

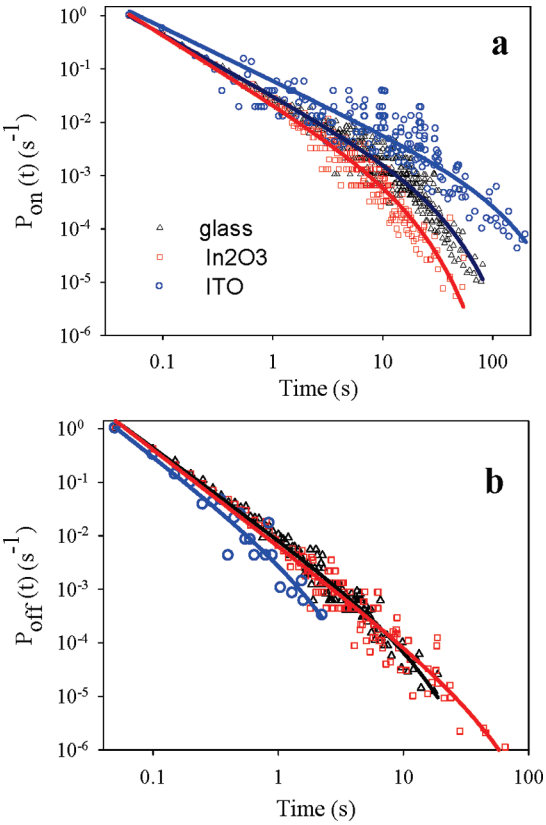

Figure 3. Normalized probability density of (a) on states ($P_{on}(t)$) and (b) off states ($P_{off}(t)$) for single QDs on ITO (blue circle), glass (black triangle), and In_2O_3 (red square). The solid lines are best fits by eq 3.

TABLE 1. Fitting Parameters of $P_{on}(t)$ and $P_{off}(t)$ for All Single QDs on Glass, In_2O_3, and ITO

	m_{on}	$1/\Gamma_{on}$ (s)	m_{off}	$1/\Gamma_{off}$ (s)
QDs on ITO	0.90 ± 0.05	84 ± 18	1.82 ± 0.3	1.7 ± 0.7
QDs on glass	1.15 ± 0.04	28 ± 3	1.70 ± 0.06	10 ± 2
QDs on In_2O_3	1.30 ± 0.05	15 ± 1	1.80 ± 0.07	39 ± 14

and Γ the saturation rate. The fitting parameters are listed in Table 1. Compared to glass, single QDs on ITO have a smaller Γ_{on} and larger Γ_{off}, suggesting increased probability densities of long on events and decreased probability densities of long off events. In fact, no off events with durations of longer than 3 s were observed for QDs on ITO. In contrast, single QDs on In_2O_3 show smaller probability of long on events and a slightly larger probability of long (>10 s) off events than those on glass.

To ensure that these single QDs are representative of the ensembles, we have also measured ensemble-averaged fluorescence decays of QDs on glass, In_2O_3, and ITO. The ensemble measurements were conducted by using samples with a QD coverage level ~10^4 times higher than those in single QD measurements. To avoid repetitive illumination of the same QDs, the samples were raster scanned at a speed of ~100 nm/s during the measurement. As shown in Figure 4, ensemble-averaged fluorescence decays of QDs on these substrates follow the same trend of decay rates as observed in single QD measurements. For a QD on glass and In_2O_3, the sum of single QD decays agrees well with the ensemble-averaged decays at long delay times (>4 ns) but shows a larger amplitude at early delay time, as shown in Figure S2 (Supporting Information). The difference is more pronounced on In_2O_3 than glass. Similar differences between the sum of single QDs and ensemble-averaged measurement were observed in our previous comparison of QDs on TiO_2.[36] Under single QD conditions, the repetitive illumination leads to the charging of QDs,[6,12,16] which results in a larger amplitude of fast decay components (due to Auger relaxation

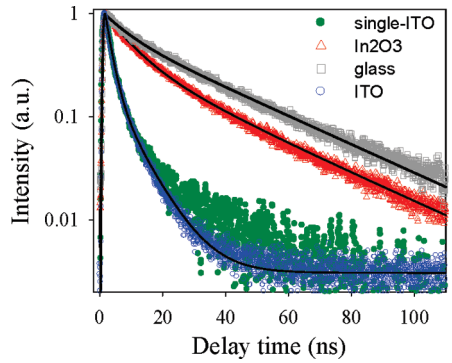

Figure 4. Ensemble-averaged fluorescence decays of QDs on ITO (blue open circles), glass (gray squares), and In_2O_3 (red triangles). Solid lines are best biexponential fits. The fluorescence decay of the sum of all single QDs on ITO (green filled circles) is also shown.

in charge particles) than the ensemble decay kinetics. In contrast, For QDs on ITO, the sum of single QD decays agrees well with the ensemble-averaged decay, consistent with the much smaller off-state contribution in the single QD trajectories. These curves show a slight difference in long delay times. The reason for this difference is unclear. It may result from the lower signal-to-noise level of the single QD data. The comparison presented here confirms that the observed single QDs are representative of the whole ensembles on these substrates. The decay curves shown in Figure 4 can be well fit by biexponential functions. The time constants and amplitudes (in parentheses) are 7.5 ns (36%) and 31.5 ns (74%) on glass, 7.6 ns (61%) and 29.1 ns (39%) on In_2O_3, and 2.0 ns (85%) and 8.7 ns (15%) on ITO. The data on ITO show a long-lived (≫100 ns) component with 0.2% of the total amplitude, which has been attributed to the background signal. The amplitude weighted average time constants are 22.9 ns on glass, 16.0 ns on In_2O_3, and 3.0 ns on ITO.

The $CdSe/CdS_{3ML}ZnCdS_{2ML}ZnS_{2ML}$ QDs used in this study have a first exciton peak at 605 nm, which is red-shifted from the first exciton peak (574 nm) of the CdSe core. The estimated radius of the CdSe core is 1.8 nm.[42] Effective mass model calculations of CdSe/CdS core/shell structures show that the lowest energy conduction band electron is delocalized in the core and shell, whereas the valence band hole remains localized in the core.[43,44] We attribute the red shift of the exciton peak position in our core/multishell structure to the lowering of the conduction band electron energy relative to the CdSe core. The estimated oxidation and reduction potentials of the 1S exciton in the core/multishell structure are −0.85 and +1.05 V (*vs* SCE), respectively.[45−47] The conduction and valence band potentials of In_2O_3 at pH 7 are at −0.4 and 2.1 V (*vs* SCE), respectively.[48] As shown in Figure 5a, the offset of conduction band edge positions in In_2O_3 and QD should enable photoinduced electron transfer from excited QDs to In_2O_3. ET from dye molecules (with excited-state potentials similar to the QDs) to In_2O_3 nanocrystalline thin films has been observed previously.[49,50] ET from CdSe QDs to TiO_2, whose conduction band edge is ~0.5 V higher than In_2O_3, has also been reported and verified in $CdSe/TiO_2$-based solar cells.[4,51−54] For these reasons, we attribute the shorter lifetimes of QDs on In_2O_3 to quenching by ET to In_2O_3. From the measured fluorescence lifetimes on glass and In_2O_3, an average ET rate from QDs to In_2O_3 can be estimated to be 1.9×10^7 s^{-1}. This ET rate is similar to those for the same QDs on TiO_2.[36] ET rate from CdSe core-only QDs (capped by mercaptopropionic acid) to TiO_2 nanoparticles was reported to be 6.3×10^7 and 6.7×10^8 s^{-1} for QDs with a first exciton peak at 605 and 570 nm, respectively.[55] In our core/multishell QDs, ZnS and CdZnS shells likely present a tunneling barrier for ET from the core because their conduction band edges are higher than CdS and CdSe.[56,57] In com-

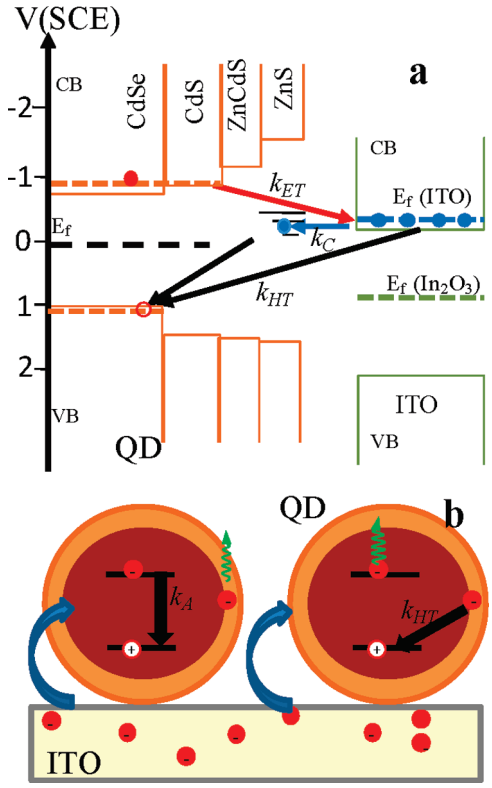

Figure 5. (a) Schematic of relevant energy levels for possible charge transfer pathways between QDs and ITO and In_2O_3; k_{ET} indicates the rate of electron transfer from QDs to ITO (or In_2O_3). Values of k_{HT} and k_c indicate the rate of hole transfer and charging of QDs on ITO, respectively. (b) Proposed exciton Auger recombination and hole transfer processes in negatively charged QDs on ITO.

parison to the core-only QDs,[55] the slower ET rate from our core/multishell QD may be attributed to the presence of the CdZnS and ZnS shells and different surface ligands. In addition, the comparison of blinking dynamics shows that single QDs on In_2O_3 blink more frequently and have lower probability of long on states than those on glass. The effect of In_2O_3 on the blinking dynamics of a QD is similar to those of TiO_2 and has been attributed to the presence of interfacial ET process.[36]

The conduction and valence band potentials for ITO are similar to those for In_2O_3.[48] Their Fermi levels are different, as shown in Figure 5a. The electron density for a 10% doped ITO has been estimated to be ~2.2 × 10^{21} cm^{-3}.[58] The Fermi level of the ITO film could then be calculated by[59]

$$E_f = E_i + kT\ln\left(\frac{N}{N_i}\right) \quad (4)$$

where E_f and E_i and $N(N_i)$ are the Fermi energy and conduction band electron density, respectively, of the doped (intrinsic) semiconductor, k is the Boltzmann constant, and T is the temperature. E_i is assumed to be at the middle of the band gap for In_2O_3 and is given by[60]

$$N_i(T) = 2.5\left(\frac{m_c m_v}{m_0^2}\right)^{3/4}\left(\frac{T}{300\ \mathrm{K}}\right)^{3/2}\exp\left(-\frac{E_g}{2kT}\right)10^{19}\ \mathrm{cm}^{-3} \quad (5)$$

where E_g is the band gap energy of the semiconductor, m_c and m_v are the effective mass of the conduction band electron and valence band hole, respectively, and m_0 is the mass of free electrons. Taking E_g = 2.5 eV,[48] $m_c = 0.3m_0$, $m_v = 0.6m_0$ for In_2O_3,[61] we calculated N_i to be ~4.95 × 10^{-3} cm^{-3} at 298 K. Taking E_i = ~0.9 eV (*vs* SCE), $N = 2.2 \times 10^{21}$ cm^{-3}, we estimate the Fermi level of ITO, E_f, to be ~100 meV higher than its conduction band edge.

Because the Fermi level in ITO is close to its conduction band edge, only states near the band edge are filled. Most conduction band states are unoccupied and the density of electron accepting states for ET from QDs should not be significantly smaller than QD/In_2O_3. For this reason, we assume that the ET rate from QDs to ITO is similar to that in QD/In_2O_3. This assumption is validated by a previous study of ET from adsorbed molecules to ATO (Sb doped SnO_2), in which it was shown that the ET rate was independent of the doping levels and was similar to that in undoped SnO_2.[62] However, the observed average lifetime for QDs on ITO is significantly faster than that on In_2O_3, suggesting that the fast quenching of QD excitons cannot be attributed to ET from QDs to ITO.

The n-doped ITO provides two additional nonradiative quenching pathways that are not available on In_2O_3 or glass. Because of the higher Fermi level in ITO than QDs, when they come in contact, electrons in ITO will be transferred to QDs until their Fermi levels are equilibrated. As a result, QDs will become negatively charged. A recent study of the fluorescence decays of CdSe/CdS core/shell QDs on ITO showed that their fluorescence lifetime decreased with increased negative bias, from which the lifetimes of negatively charged QDs were determined to be 700−1500 ps.[38] It was suggested that optical excitation of these negatively charged QDs formed negative trions (an exciton and an electron), whose lifetimes were shorter than single excitons in neutral QDs due to the presence of the Auger relaxation pathway involving the additional electron. Although the radiative rate of the trions is a factor two faster than single excitons, the main effect of the extra electron is the enhancement of its exciton Auger recombination rate. Under our experimental conditions, there is no applied external bias, and the initial Fermi level of ITO is below the conduction band edge of CdSe/ZnS QDs. The electrons in the negatively charged QDs likely fill in the trap states below the conduction band edge. We speculate that these trapped electrons can also provide fast nonradiative decay pathways for quenching the QD emission. As shown in Figure 5b, they can facilitate the nonradiative exciton recombination and/or

combine with the valence band holes, both of which reduce the exciton lifetime. The observed average lifetime for QDs on ITO is about 3 ns, suggesting that these nonradiative decay processes involving trapped electrons are slightly slower than those reported for negative trions.[38]

Unlike on In_2O_3 and glass, single QDs on ITO show narrow distributions of lifetimes and suppressed blinking activity with negligible contribution of off states. It is believed that, in the off state, QDs are charged and its excitons are nonemissive due to a fast Auger relaxation process involving the additional charge.[7−31] A direct measurement of QDs under optical illumination shows that QDs become positively charged.[8] A recent study of the lifetime and emission of intensity of negative trions shows that negatively charged QDs are optically bright and cannot account for the off state of single QDs.[38] These studies suggest that in off states QDs are positively charged. For the QDs on ITO, the holes are short-lived due to fast hole transfer processes to either the trapped electrons in the negatively charged QD or to ITO, inhibiting the formation of the off state. It should be noted that suppression of blinking has also been reported for QDs in reducing solution environments, which also provide electron sources to remove any long-lived holes in the QD.[28,30] Furthermore, in contact with the ITO, the charges of the QDs are likely maintained at a constant level because of Fermi level equilibration. For this reason, charging induced nonradiative decays should remain constant, which may be the reason for the small variations of intensity and lifetime throughout the trajectories and among different QDs on ITO.

Suppression of blinking and reduction of lifetime have also been observed for single QDs on metal substrates.[26,34,63] Shimizu *et al.* showed that, for CdSe/ZnS core/shell QDs on rough Au films, the reduction of lifetime is accompanied by an increase of fluorescence intensity, suggesting an enhancement of radiative decay and excitation rates, due to the enhanced local electric field.[26] They attribute the suppression of QD blinking to effective competition of the enhanced radiative process with exciton Auger recombination in charged QDs. This model is further supported by the observation that single QDs switch between two emission wavelengths, indicating the presence of two charge states. Similar blinking suppression and fluorescence enhancement of single QDs on rough Au films were observed in a more recent study by Ito and co-workers, although a different model for the blinking suppression was proposed.[63] This study showed that on flat Au films single QDs also show suppressed blinking. In addition, both fluorescence lifetime and intensity are reduced. It was suggested that for single QDs on metal surfaces the suppression of blinking is due to a fast removal of charges from QDs by charge transfer to and from the metal substrate, and the reduction of lifetime is caused by energy transfer. In our model, we also assume a fast removal of holes in QDs. However, we suggest that the fast charge transfer between QDs and ITO should lead to the equilibration of their Fermi levels and the formation of negatively charged QDs. We attribute the reduction of lifetime and fluorescence intensity to the fast exciton Auger recombination[38] and hole transfer in negatively charged QDs.

CONCLUSIONS

The exciton quenching dynamics of single CdSe/$CdS_{3ML}ZnCdS_{2ML}ZnS_{2ML}$ core/multishell QDs adsorbed on glass, In_2O_3, and ITO have been compared. A good agreement of the average fluorescence lifetimes determined by single QDs and ensemble-averaged measurements on these substrates is observed, suggesting that the single QDs studied are representative of the ensembles. Single QDs on In_2O_3 show shorter fluorescence lifetimes and higher blinking frequencies than those on glass. These differences can be attributed to the presence of interfacial ET from QDs to In_2O_3 and are consistent with previous findings of single QDs on TiO_2. In comparison to glass and In_2O_3, single QDs on ITO show suppressed blinking activity as well as reduced and more narrowly distributed fluorescence lifetimes and intensity. Due to the high doping level in ITO, the equilibration of the Fermi levels of QDs and ITO leads to the formation of negatively charged QDs. We speculate that the exciton Auger recombination and hole transfer processes in these negatively charged QDs shorten their fluorescence lifetime and suppress their blinking activities. This study shows that the blinking of single QDs can be effectively suppressed on the surface of ITO. This phenomenon may also be observable for other QDs and on different n-doped semiconductors.

METHODS

Materials. CdSe/$CdS_{3ML}ZnCdS_{2ML}ZnS_{2ML}$ core/multishell QDs (capped by octadecylamine ligand, first exciton absorption peak at 605 nm) were obtained from Ocean NanoTech, LLC, USA. Their absorption and emission spectra are shown in Figure S1a (Supporting Information). ITO-coated coverslips (15−30 ohms, 18 × 18 mm^2, ~10% doping) were purchased from SPI Supplies. Heptane (99%) and 2-propanol (99.5%) were purchased from Sigma Aldrich and used without further purification. Glass coverslips (25 × 25-1 mm) were purchased from Fisher Scientific.

Sample Preparation. The ITO films were first washed by 2-propanol, dried in air, and rapidly scanned over a flame for a few seconds to remove any adsorbed organic materials before use. The flame treatment process did not change the resistance of ITO. In_2O_3 nanocrystalline thin films on glass coverslips were

prepared according to a reported procedure.[49] To prepare samples for single QD study, a QD heptane solution with a concentration of ~10 pM was spin-coated on ITO, In_2O_3, or glass coverslips. For ensemble-averaged measurement, the samples were prepared by spin-coating a QD solution with a concentration of ~0.1 μM.

Instruments. Both single QD and ensemble-averaged measurements were carried out with a home-built scanning confocal microscope. Femtosecond laser pulses (~100 fs) with a repetition rate of 80 MHz were generated with a mode-locked Ti:sapphire laser (Tsunami oscillator pumped by 10 W Millennia Pro, Spectra-Physics). The output centered at 1000 nm was passed through a pulse picker (Conoptics, USA) to reduce the repetition rate by a factor of 9 and then frequency doubled in a BBO crystal to generate 500 nm excitation pulses. The coverslips (glass, ITO, or In_2O_3) containing QDs were placed on a piezo scanner (Mad City Laboratories). The excitation beam (~150 nW) was focused through an objective (100×, NA 1.4, oil immersion, Olympus) down to a diffraction-limited spot on the sample. The resulting epifluorescence from the sample was detected by an avalanche photodiode (APD, Perkin-Elmer SPCM-AQR-14). The APD output was analyzed by a time-correlated single photon counting (TC-SPC) board (Becker&Hickel SPC 600). The instrument response function for the fluorescence lifetime measurement had a full width at half-maximum of ~500 ps. In both single particle and ensemble-averaged measurements, QD fluorescence between 540 and 675 nm was selected by a band-pass filter for detection. A typical raster scanned fluorescence image of single QDs on ITO is shown in Figure S1b (Supporting Information).

Acknowledgment. The work was supported by the National Science Foundation under Grant No. CHE-0848556 and the Petroleum Research Fund (PRF #49286-ND6).

Supporting Information Available: Absorption and emission spectra, single QD image, comparison of single QD and ensemble-averaged fluorescence decays on ITO and glass, single QD fluorescence intensity and lifetime trajectories on ITO and In_2O_3, and a representative single QD fluorescence decay and single exponential fit. This material is available free of charge *via* the Internet at http://pubs.acs.org.

REFERENCES AND NOTES

1. Colvin, V. L.; Schlamp, M. C.; Alivisatos, A. P. Light-Emitting Diodes Made from Cadmium Selenide Nanocrystals and a Semiconducting Polymer. *Nature* **1994**, *370*, 354–357.
2. Coe, S.; Woo, W.-K.; Bawendi, M. G.; Bulović, V. Electroluminescence from Single Monolayers of Nanocrystals in Molecular Organic Devices. *Nature* **2002**, *420*, 800–803.
3. Huynh, W. U.; Dittmer, J. J.; Alivisatos, A. P. Hybrid Nanorod-Polymer Solar Cells. *Science* **2002**, *295*, 2425–2427.
4. Robel, I.; Subramanian, V.; Kuno, M.; Kamat, P. V. Quantum Dot Solar Cells. Harvesting Light Energy with CdSe Nanocrystals Molecularly Linked to Mesoscopic TiO2 Films. *J. Am. Chem. Soc.* **2006**, *128*, 2385–2393.
5. Shalom, M.; R|Aauhle, S.; Hod, I.; Yahav, S.; Zaban, A. Energy Level Alignment in CdS Quantum Dot Sensitized Solar Cells Using Molecular Dipoles. *J. Am. Chem. Soc.* **2009**, *131*, 9876–9877.
6. Efros, A. L.; Rosen, M. Random Telegraph Signal in the Photoluminescence Intensity of a Single Quantum Dot. *Phys. Rev. Lett.* **1997**, *78*, 1110–1113.
7. Shimizu, K. T.; Neuhauser, R. G.; Leatherdale, C. A.; Empedocles, S. A.; Woo, W. K.; Bawendi, M. G. Blinking Statistics in Single Semiconductor Nanocrystal Quantum Dots. *Phys. Rev. B* **2001**, *63*, 205316/1–205316/5.
8. Krauss, T. D.; O'Brien, S.; Brus, L. E. Charge and Photoionization Properties of Single Semiconductor Nanocrystals. *J. Phys. Chem. B* **2001**, *105*, 1725–1733.
9. Nirmal, M.; Dabbousi, B. O.; Bawendi, M. G.; Macklin, J. J.; Trautman, J. K.; Harris, T. D.; Brus, L. E. Fluorescence Intermittency in Single Cadmium Selenide Nanocrystals. *Nature* **1996**, *383*, 802–804.
10. Empedocles, S.; Bawendi, M. Spectroscopy of Single CdSe Nanocrystallites. *Acc. Chem. Res.* **1999**, *32*, 389–396.
11. Fisher, B. R.; Eisler, H.-J.; Stott, N. E.; Bawendi, M. G. Emission Intensity Dependence and Single-Exponential Behavior in Single Colloidal Quantum Dot Fluorescence Lifetimes. *J. Phys. Chem. B* **2004**, *108*, 143–148.
12. Chung, I.; Bawendi, M. G. Relationship between Single Quantum-Dot Intermittency and Fluorescence Intensity Decays from Collections of Dots. *Phys. Rev. B* **2004**, *70*, 165304/1–165304/5.
13. Kuno, M.; Fromm, D. P.; Johnson, S. T.; Gallagher, A.; Nesbitt, D. J. Modeling Distributed Kinetics in Isolated Semiconductor Quantum Dots. *Phys. Rev. B* **2003**, *67*, 125304/1–125304/15.
14. Kuno, M.; Fromm, D. P.; Hamann, H. F.; Gallagher, A.; Nesbitt, D. J. "On"/"Off" Fluorescence Intermittency of Single Semiconductor Quantum Dots. *J. Chem. Phys.* **2001**, *115*, 1028–1040.
15. Kuno, M.; Fromm, D. P.; Gallagher, A.; Nesbitt, D. J.; Micic, O. I.; Nozik, A. J. Fluorescence Intermittency in Single InP Quantum Dots. *Nano Lett.* **2001**, *1*, 557–564.
16. Peterson, J. J.; Nesbitt, D. J. Modified Power Law Behavior in Quantum Dot Blinking: A Novel Role for Bi-excitons and Auger Ionization. *Nano Lett.* **2009**, *9*, 338–345.
17. Zhang, K.; Chang, H.; Fu, A.; Alivisatos, A. P.; Yang, H. Continuous Distribution of Emission States from Single CdSe/ZnS Quantum Dots. *Nano Lett.* **2006**, *6*, 843–847.
18. Pelton, M.; Smith, G.; Scherer, N. F.; Marcus, R. A. Evidence for a Diffusion-Controlled Mechanism for Fluorescence Blinking of Colloidal Quantum Dots. *Proc. Natl. Acad. Sci. U.S.A.* **2007**, *104*, 14249–14254.
19. Tang, J.; Marcus, R. A. Determination of Energetics and Kinetics from Single-Particle Intermittency and Ensemble-Averaged Fluorescence Intensity Decay of Quantum Dots. *J. Chem. Phys.* **2006**, *125*, 044703/1–044703/8.
20. Tang, J.; Marcus, R. A. Mechanisms of Fluorescence Blinking in Semiconductor Nanocrystal Quantum Dots. *J. Chem. Phys.* **2005**, *123*, 054704/1–054704/12.
21. Tang, J.; Marcus, R. A. Diffusion-Controlled Electron Transfer Processes and Power-Law Statistics of Fluorescence Intermittency of Nanoparticles. *Phys. Rev. Lett.* **2005**, *95*, 107401/1–107401/4.
22. Tang, J.; Marcus, R. A. Single Particle *versus* Ensemble Average: From Power-Law Intermittency of a Single Quantum Dot to Quasistretched Exponential Fluorescence Decay of an Ensemble. *J. Chem. Phys.* **2005**, *123*, 204511/1–204511/6.
23. Issac, A.; von Borczyskowski, C.; Cichos, F. Correlation between Photoluminescence Intermittency of CdSe Quantum Dots and Self-Trapped States in Dielectric Media. *Phys. Rev. B* **2005**, *71*, 161302/1–161302/4.
24. Schlegel, G.; Bohnenberger, J.; Potapova, I.; Mews, A. Fluorescence Decay Time of Single Semiconductor Nanocrystals. *Phys. Rev. Lett.* **2002**, *88*, 137401-1.
25. Verberk, R.; van Oijen, A. M.; Orrit, M. Simple Model for the Power-Law Blinking of Single Semiconductor Nanocrystals. *Phys. Rev. B* **2002**, *66*, 233202/1–233202/4.
26. Shimizu, K. T.; Woo, W. K.; Fisher, B. R.; Eisler, H. J.; Bawendi, M. G. Surface-Enhanced Emission from Single Semiconductor Nanocrystals. *Phys. Rev. Lett.* **2002**, *89*, 117401/1–117401/4.
27. Chen, Y.; Vela, J.; Htoon, H.; Casson, J. L.; Werder, D. J.; Bussian, D. A.; Klimov, V. I.; Hollingsworth, J. A. "Giant" Multishell CdSe Nanocrystal Quantum Dots with Suppressed Blinking. *J. Am. Chem. Soc.* **2008**, *130*, 5026–5027.
28. Fomenko, V.; Nesbitt, D. J. Solution Control of Radiative and Nonradiative Lifetimes: A Novel Contribution to Quantum Dot Blinking Suppression. *Nano Lett.* **2008**, *8*, 287–293.
29. Mahler, B.; Spinicelli, P.; Buil, S.; Quelin, X.; Hermier, J.-P.; Dubertret, B. Towards Non-blinking Colloidal Quantum Dots. *Nat. Mater.* **2008**, *7*, 659–664.

30. Hohng, S.; Ha, T. Near-Complete Suppression of Quantum Dot Blinking in Ambient Conditions. *J. Am. Chem. Soc.* **2004**, *126*, 1324–1325.
31. Wang, X.; Ren, X.; Kahen, K.; Hahn, M. A.; Rajeswaran, M.; Maccagnano-Zacher, S.; Silcox, J.; Cragg, G. E.; Efros, A. L.; Krauss, T. D. Non-blinking Semiconductor Nanocrystals. *Nature* **2009**, *459*, 686–689.
32. Odoi, M. Y.; Hammer, N. I.; Early, K. T.; McCarthy, K. D.; Tangirala, R.; Emrick, T.; Barnes, M. D. Fluorescence Lifetimes and Correlated Photon Statistics from Single CdSe/Oligo(phenylene vinylene) Composite Nanostructures. *Nano Lett.* **2007**, *7*, 2769–2773.
33. Hammer, N. I.; Early, K. T.; Sill, K.; Odoi, M. Y.; Emrick, T.; Barnes, M. D. Coverage-Mediated Suppression of Blinking in Solid State Quantum Dot Conjugated Organic Composite Nanostructures. *J. Phys. Chem. B* **2006**, *110*, 14167–14171.
34. Ray, K.; Badugu, R.; Lakowicz, J. R. Metal-Enhanced Fluorescence from CdTe Nanocrystals: A Single-Molecule Fluorescence Study. *J. Am. Chem. Soc.* **2006**, *128*, 8998–8999.
35. Issac, A.; Jin, S.; Lian, T. Intermittent Electron Transfer Activity from Single CdSe/ZnS QDs. *J. Am. Chem. Soc.* **2008**, *130*, 11280–11281.
36. Jin, S.; Lian, T. Electron Transfer Dynamics from Single CdSe/ZnS Quantum Dots to TiO_2 Nanoparticles. *Nano Lett.* **2009**, *9*, 2448–2454.
37. Cui, S.-C.; Tachikawa, T.; Fujitsuka, M.; Majima, T. Interfacial Electron Transfer Dynamics in a Single CdTe Quantum Dot-Pyromellitimide Conjugate. *J. Phys. Chem. C* **2008**, *112*, 19625–19634.
38. Jha, P. P.; Guyot-Sionnest, P. Trion Decay in Colloidal Quantum Dot. *ACS Nano* **2009**, *3*, 1011–1015.
39. Wang, S.; Querner, C.; Emmons, T.; Drndic, M.; Crouch, C. H. Fluorescence Blinking Statistics from CdSe Core and Core/Shell Nanorods. *J. Phys. Chem. B* **2006**, *110*, 23221–23227.
40. Mandal, A.; Nakayama, J.; Tamai, N.; Biju, V.; Isikawa, M. Optical and Dynamic Properties of Water-Soluble Highly Luminescent CdTe Quantum Dots. *J. Phys. Chem. B* **2007**, *111*, 12765–12771.
41. Durisic, N.; Wiseman, P. W.; Grutter, P.; Heyes, C. D. A Common Mechanism Underlies the Dark Fraction Formation and Fluorescence Blinking of Quantum Dots. *ACS Nano* **2009**, *3*, 1167–1175.
42. Yu, W. W.; Qu, L.; Guo, W.; Peng, X. Experimental Determination of the Extinction Coefficient of CdTe, CdSe, and CdS Nanocrystals. *Chem. Mater.* **2003**, 2854–2860.
43. Garcia-Santamaria, F.; Chen, Y.; Vela, J.; Schaller, R. D.; Hollingsworth, J. A.; Klimov, V. I. Suppressed Auger Recombination in "Giant" Nanocrystals Boosts Optical Gain Performance. *Nano Lett.* **2009**, *9*, 3482–3488.
44. Pandey, A.; Guyot-Sionnest, P. Intraband Spectroscopy and Band Offsets of Colloidal II−VI Core/Shell Structures. *J. Chem. Phys.* **2007**, *127*, 104710/1–104710/10.
45. Huang, J.; Stockwell, D.; Huang, Z.; Mohler, D. L.; Lian, T. Photoinduced Ultrafast Electron Transfer from CdSe Quantum Dots to Re-Bipyridyl Complexes. *J. Am. Chem. Soc.* **2008**, *130*, 5632–5633.
46. Brus, L. A Simple Model for the Ionization Potential, Electron Affinity, and Aqueous Redox Potentials of Small Semiconductor Crystallites. *J. Chem. Phys.* **1983**, *79*, 5566–5571.
47. Brus, L. E. Electron−Electron and Electron−Hole Interactions in Small Semiconductor Crystallites: The Size Dependence of the Lowest Excited Electronic State. *J. Chem. Phys.* **1984**, *80*, 4403–4409.
48. Erbs, W.; Kiwi, J.; Gratzel, M. Light-Induced Oxygen Generation in Aqueous Dispersion of Indium Oxide (In_2O_3) Particles and Determination of Their Conduction Band Position. *Chem. Phys. Lett.* **1984**, *110*, 648–650.
49. Guo, J.; Stockwell, D.; Ai, X.; She, C.; Anderson, N. A.; Lian, T. Electron-Transfer Dynamics from Ru Polypyridyl Complexes to In_2O_3 Nanocrystalline Thin Films. *J. Phys. Chem. B* **2006**, *110*, 5238–5244.
50. Huang, J.; Stockwell, D.; Boulesbaa, A.; Guo, J.; Lian, T. Comparison of Electron Injection Kinetics from Rhodamine B to In_2O_3, SnO_2 and ZnO Nanocrystalline Thin Films. *J. Phys. Chem. C* **2008**, *112*, 5203–5212.
51. Lee, H. J.; Yum, J.-H.; Leventis, H. C.; Zakeeruddin, S. M.; Haque, S. A.; Chen, P.; Seok, S. I.; Grätzel, M.; Nazeeruddin, M. K. CdSe Quantum Dot-Sensitized Solar Cells Exceeding Efficiency 1% at Full-Sun Intensity. *J. Phys. Chem. C* **2008**, *112*, 11600–11608.
52. Chakrapani, V.; Tvrdy, K.; Kamat, P. V. Modulation of Electron Injection in CdSe-TiO_2 System through Medium Alkalinity. *J. Am. Chem. Soc.* **2010**, *132*, 1228–1229.
53. Robel, I.; Subramanian, V.; Kuno, M.; Kamat, P. V. Quantum Dot Solar Cells. Havesting Light Energy with CdSe Nanocrystals Molecularly Linked to Mesoscppic TiO_2 Films. *J. Am. Chem. Soc.* **2006**, *128*, 2385–2393.
54. Robel, I.; Kuno, M.; Kamat, P. V. Size-Dependent Electron Injection from Excited CdSe Quantum Dots into TiO_2 Nanoparticles. *J. Am. Chem. Soc.* **2007**, *129*, 4136–4137.
55. Kongkanand, A.; Tvrdy, K.; Takechi, K.; Kuno, M.; Kamat, P. V. Quantum Dot Solar Cells. Tuning Photoresponce through Size and Shape Control of CdSe−TiO_2 Architecture. *J. Am. Chem. Soc.* **2008**, *130*, 4007–4015.
56. Talapin, D. V.; Mekis, I.; Gotzinger, S.; Kornowski, A.; Benson, O.; Weller, H. CdSe/CdS/ZnS and CdSe/ZnSe/ZnS Core/Shell/Shell Nanocrystals. *J. Phys. Chem. B* **2004**, *108*, 18826–18831.
57. Xie, R.; Kolb, U.; Li, J.; Basche, T.; Mews, A. Synthesis and Characterization of Highly Luminescent CdSe−Core CdS/$Zn_{0.5}Cd_{0.5}S$/ZnS Multishell Nanocrystals. *J. Am. Chem. Soc.* **2005**, *127*, 7480–7488.
58. Brewer, S. H.; Franzen, S. Calculation of the Electronic and Optical Properties of Indium Tin Oxide by Density Functional Theory. *Chem. Phys.* **2004**, *300*, 285–293.
59. Hunter, L. P. *Introduction to Semiconductor Phenomena and Devices*; Addison-Wesley: Reading, MA, 1996; p 31.
60. Ashcroft, N. W.; Mermin, N. D. *Solid State Physics*; Thomson Learning: New York, 1976.
61. Hamberg, I.; Granqvist, C. G. Evaporated Tin-Doped Indium Oxide Films: Basic Optical Properties and Applications to Energy-Efficient Windows. *J. Appl. Phys.* **1986**, *60*, R123–R159.
62. Guo, J.; She, C.; Lian, T. Ultrafast Electron Transfer between Molecule Adsorbate and Antimony Doped Tin Oxide (ATO) Nanoparticles. *J. Phys. Chem. B* **2005**, *109*, 7095–7102.
63. Ito, Y.; Matsuda, K.; Kanemitsu, Y. Mechanism of Photoluminescence Enhancement in Single Semiconductor Nanocrystals on Metal Surfaces. *Phys. Rev. B* **2007**, *75*, 033309/1–033309/4.